

# Dimensional stability testing in thermal vacuum of the CHEOPS optical telescope assembly

W.A. Klop<sup>1</sup>, A.L. Verlaan<sup>2</sup>

TNO, Institute of applied physics, Stieltjesweg 1, 2628 CK, The Netherlands,  
wimar.klop@tno.nl<sup>1</sup>, ad.verlaan@tno.nl<sup>2</sup>

## ABSTRACT

The CHEOPS mission (CHaracterising ExOPlanet Satellite) is dedicated to searching for exoplanetary transits by performing ultra-high precision photometry on bright stars already known to host planets. A 32cm diameter on-axis Ritchey-Chrétien telescope is used for imaging onto a single cooled detector. With integration times up to 48 hours the thermal stability of the telescope and its structure are key to the performance. Using a multi-lateration interferometer setup TNO has successfully demonstrated the  $\mu\text{m}$ -level stability of the Structural Thermal Model (STM2) of the Optical Telescope Assembly (OTA) in thermal vacuum. This OTA was later upgraded to become the Flight Model. Experiments comprise thermal vacuum cycling, thermal vacuum stability testing where axial and lateral deformations are measured to the nm-level sensitivity.

**Keywords:** CHEOPS, Optical Telescope Assembly, thermal stability, thermal vacuum facility

## 1. INTRODUCTION

The CHaracterising ExOPlanet Satellite (CHEOPS) [1] is a mission defined by ESA and led by Bern University (Switzerland) to search for transits on bright stars that are known to host planets. CHEOPS will focus on exoplanets with a structural radii in the range of 1-6  $R_{\text{Earth}}$ . The measurement principle is based on photometric signals with a precision limited by stellar photon noise of 150 ppm/min for a 9<sup>th</sup> magnitude star. The design of the instrument is based on a Ritchey-Chretien style telescope with an aperture of 32 cm. The photons collected by the telescope are collected by a single frame-transfer backside illuminated CCD detector located in the focal plane assembly.

The telescope and optical telescope assembly (OTA) are two key components produced by Almatech (Switzerland). To enable the mission requirements for CHEOPS the stability with respect to temperature is required to be within about 1 $\mu\text{m}$  and 10 $\mu\text{rad}$  within the operational temperature range of -5 to +5°C. The thermo-mechanical stability of the telescope assembly is verified experimentally in a thermal vacuum chamber by TNO (Delft, The Netherlands). To enable the experiment a verification setup is designed and realized, combining interferometric length metrology with a controlled thermal shroud in vacuum. The design of the setup was based on the LISA (Laser Interferometer Space Antenna) Optical Characterizations project [1], which had similar measurement requirements. That project, executed from 2012 to 2014 for ESA, successfully demonstrated the feasibility to realize and validate the thermo-mechanical performance of a telescope assembly for the LISA mission.

This paper addresses the design, realization and validation of the experimental setup itself and concludes by providing an overview of the executed experiment on the CHEOPS STM. The paper is organized as follows; First the telescope assembly is briefly discussed. Second the thermal vacuum setup is discussed. In the next section description is provided on the design and operation of the length metrology system and the interpretation of its results. Then the characterization of the test setup is described, followed by a description of the test program of the OTA. Finally the achieved results are shown to complete the test description. A more detailed explanation of the telescope design as well as the interpretation of the test results are reported in a separated paper by Almatech.

## 2. TELESCOPE ASSEMBLY STRUCTURE

The OTA structure is designed and realized by Almatech. The core material of the OTA is Carbon Fiber Reinforced Plastic (CRFP), which is used due to its high relative stiffness and the ability to trim its CTE to a desired low value. By

analytical modeling all expected load cases, the structure is designed to yield a high dimensional stability over its operational temperature range. The operational temperature ranges foreseen is divided into two cases. First a settling case were the expected temperature drop is -30K going from an ambient reference temperature of 20°C to the operational temperature of -10°C The second case is an in-orbit stability case were a delta temperature of  $\pm 5\text{K}$  around a reference temperature of -10°C is expected. In Figure 1 pictures of the OTA as tested at TNO are shown. The OTA structure sub-system provides mechanical support for a number of components. In addition the structure Sub-System provides mechanical, thermal an electrical hardware interfaces to the Telescope mirrors (M1 and M2), the Back-End Optics, including housing (BEO), the Focal Plane Module (FPM) and Two radiators

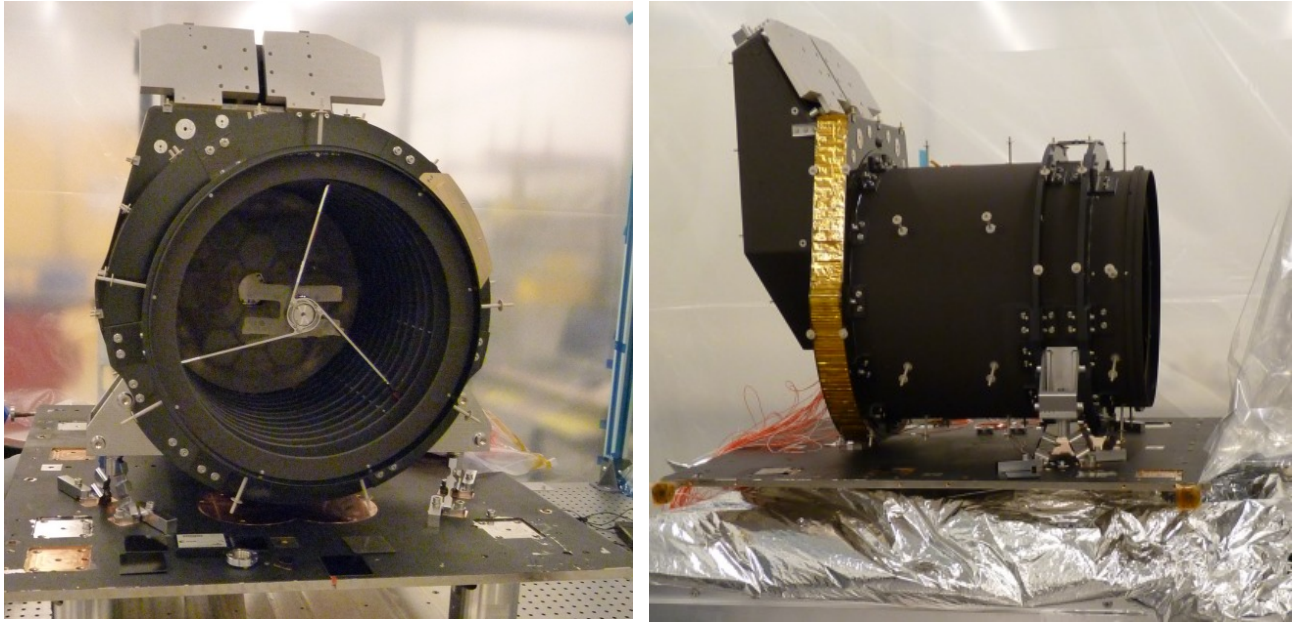


Figure 1. Impression of the CHEOPS STM Telescope assembly designed and realized by Almatech

### 3. THERMAL VACUUM CHAMBER

The Vacuum Chamber Facility (VCF) is a standard facility present at TNO offering both the ability to achieve high vacuum levels and temperature control. The temperature can be controlled on an object mounting plate and a cylindrical shroud surrounding the test object. A gas mixture system is used to control these temperatures. First it preheats liquid nitrogen to the desired set point temperature and then nitrogen in gas form is led through both the object plate and the shroud, which can be controlled separately. The resolution at which the temperatures can be set is 1K with a measurement accuracy at the object plate of approximately 0.1K.

Key point of the study at hand is the characterization and demonstration of the OTA- structure low thermal deformation. For this purpose the experimental setup has to offer an high thermal stability ( $<0.5\text{K/hr}$ ) and uniformity ( $<1\text{K}$ ). With respect to the CHEOPS STM, the VCF provides the required volume, the temperature ranges and accuracy. In addition the VCF is equipped pressure, temperature and gas composition sensing and data acquisition system.

The OTA-structure is mounted on the object plate by the usage of three struts. Both the object plate and the OTA are covered by an Multi-layer insulation (MLI) tent creating two separate temperature zones in the thermal vacuum facility. As a result the Interferometer breadboard is kept at a steady temperature of 20°C, while varying the OTA over its operational temperature range. To monitor the temperatures and its uniformity on the OTA structure, the structure is equipped with 20 thermal sensors. The sensors (3-wire PT-100's) are connected to an EuroTherm monitoring system.

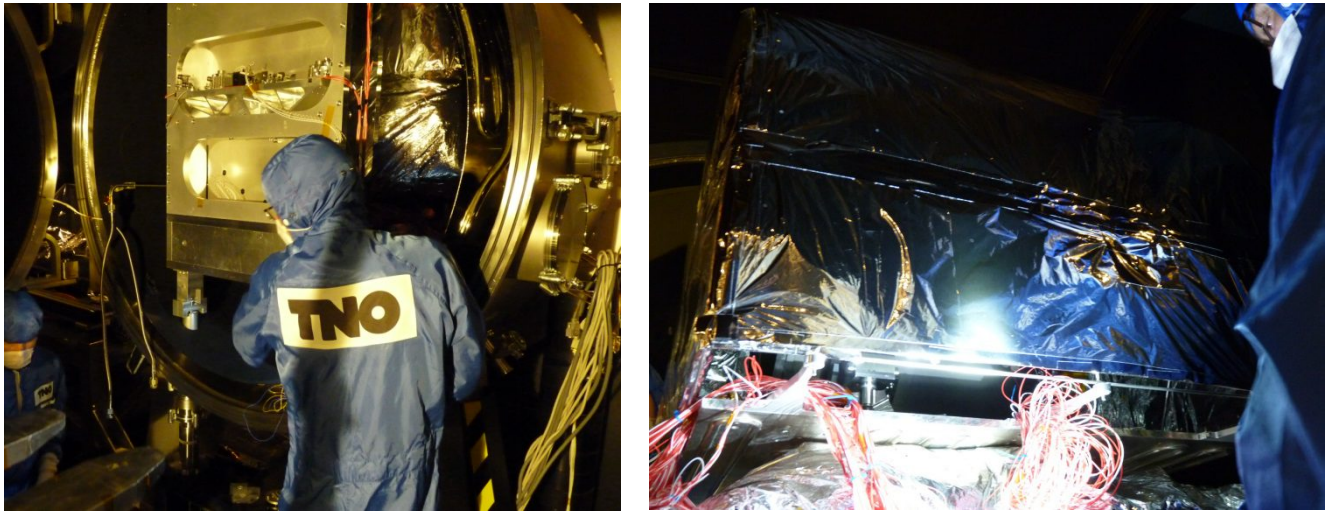


Figure 2. Left, Vacuum chamber Facility (VCF) with the build-in metrology system holding the OTA. Right, MLI tent covering the OTA structure mounted on the object plate.

#### 4. LENGTH METROLOGY SYSTEM

The core of the length metrology system consists of three relative displacement interferometers to measure the deformation of the OTA structure throughout the thermal vacuum experiments. These interferometers are placed on a very stable breadboard, mounted inside the metrology frame, in its turn inside the thermal vacuum facility. The Interferometer laser source, as well as the detectors are placed outside the vacuum, removing heat sources from the test setup inside the vacuum. Using an active beam alignment system the interferometer laser beams are maintained in auto-collimation on the M1 mirror of the OTA throughout the full experiment. Using these interferometers the displacement and rotation between the optical inserts, located at the telescope mirrors M1 and M2 are measured. This is the most direct approach to monitor the deformation of the mirrors in the telescope. Altogether distance variations are monitored between the 2 mirrors over 3 different optical paths, while minimizing the metrology complexity This measurement configuration is shown in Figure 3.

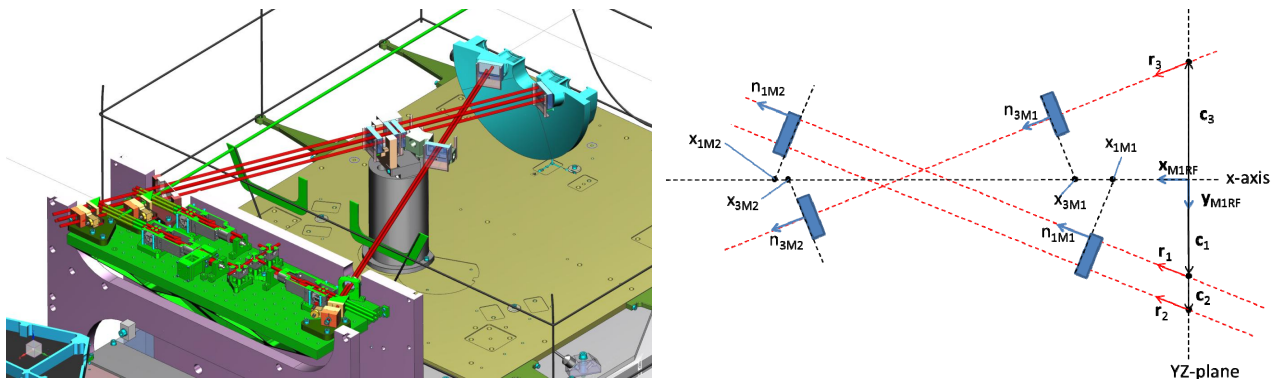


Figure 3. The left image shows a CAD impression of the metrology system. The right image shows a schematic view of the metrology system including references.

An essential part of the deformation measurement approach is the use of metrology mirrors. These metrology mirrors are based on the flight design mirrors, but are modified to enable interferometric measurements of the mirror relative displacement as shown in Figure 3. Figure 4 depicts the inserts for both the M1 as the M2. These metrology mirrors are made from Zerodur CTE class 0. To exclude thermal deformations can be introduced by these mirrors. On top the M2-

metrology mirror can be used without the actual telescope, but with the metrology mirrors. By doing so a perfect (near-zero length and near zero CTE) reference telescope can be created, making use of the same parts and interfaces. This latter configuration is applied for the reference test performed to assess the overall system accuracy over a full thermal test cycle.

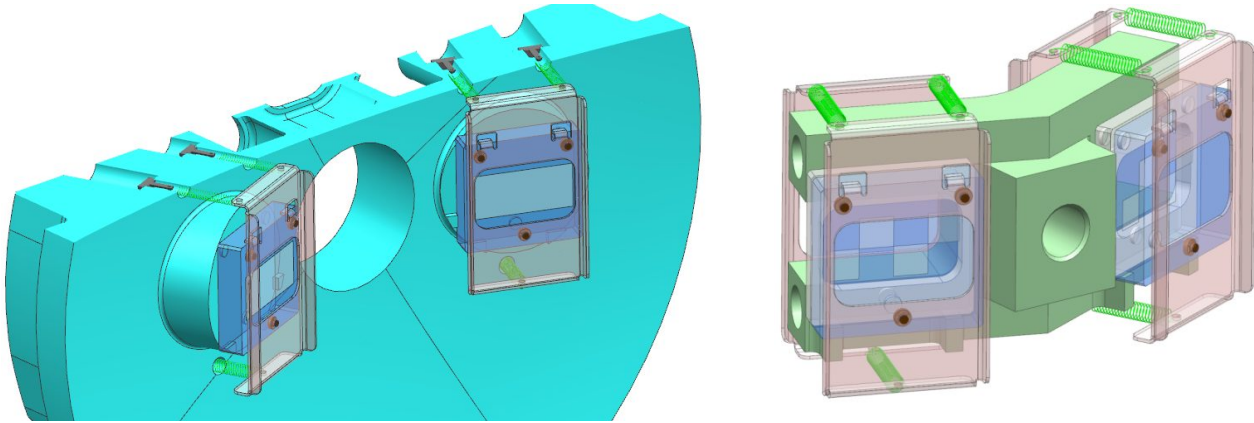


Figure 4. (left) Cross-section of the M1 metrology mirror with posts inserted in the metrology mirror. The springs that run from the posts to the pressing plate that hold the insert in place are shown in green. (Right) M2 metrology mirror with inserts mounted via springs and spring plates.

From the obtained length changes  $\delta l_1$ ,  $\delta l_2$  and  $\delta l_3$ , the telescope deformation  $\delta x$ ,  $\delta y$  and  $\delta \alpha$  can be determined. We start by assuming that the measurement system is properly aligned, meaning that the M1 insert and the M2 inserts are both perpendicular to the laser beams. We will use the so called M1RF\* reference frame.

Let's indicate the propagation direction of laser beam  $i$  going from M1 towards M2 with the unit vector  $\hat{r}_i = (r_{ix}, r_{iy}, r_{iz})$  and the normal unit vectors for the two mirrors associated with beam  $i$  with  $\hat{n}_{iM1} = (n_{iM1x}, n_{iM1y}, n_{iM1z})$  and  $\hat{n}_{iM2} = (n_{iM2x}, n_{iM2y}, n_{iM2z})$ . As interferometer 1 and 2 share the same inserts,  $\hat{n}_{2M1} = \hat{n}_{1M1}$  and  $\hat{n}_{2M2} = \hat{n}_{1M2}$ . Furthermore, the cross-point of beam  $i$  with the YZ plane is given by the vector  $\mathbf{c}_i$ . The cross-point of the M1 mirror plane associated with beam  $i$  and the X-axis is given by  $(x_{iM1}, 0, 0)$ ; The cross-point of the M2 mirror plane associated with beam  $i$  and the X-axis is given by  $(x_{iM2}, 0, 0)$ .

Using these definitions, the distance between the mirrors as measured along beam path  $i$  is

$$\Delta l_i = \frac{x_{iM2} n_{iM2x} - \hat{n}_{iM2} \cdot \mathbf{c}_i}{\hat{n}_{iM2} \cdot \hat{r}_i} - \frac{x_{iM1} n_{iM1x} - \hat{n}_{iM1} \cdot \mathbf{c}_i}{\hat{n}_{iM1} \cdot \hat{r}_i}. \quad (1)$$

Note that the above equation gives the distance between the mirrors. To get the total interferometer beam optical path difference (in double pass),  $\Delta l_i$  needs to be multiplied by four.

The next step is to calculation the change in the path length in equation (1), when M2 undergoes a defocus  $\delta x$ , a decenter  $\delta y$  and a rotation  $\delta \alpha$ . Note that in M1RF\* coordinate system only M2 changes (by definition). The orientation and position of M1 remains constant, because M1RF\* is linked to M1 in the deformed state. Furthermore, the active laser pointing control will keep the laser beam orientations perpendicular to the M1 surfaces. This leads to the following mirror separation change

$$\delta l_i = \frac{n_{iM2x} \delta x + n_{iM2y} \delta y - n_{iM2x} c_{iy} \delta \alpha}{\hat{n}_{iM2} \cdot \hat{r}_i}, \quad (2)$$

where the approximation  $\delta \alpha \ll 1$  has been used.



The inner product in the denominator of equation (2) is equal of the cosine of the beam incidence angle on M2. This incidence angle will be aligned to zero. Any misalignment will be taking into account in the error budget. Here, we will set the inner product to 1, leading to the following matrix equation for the forward model

$$\begin{pmatrix} \delta l_1 \\ \delta l_2 \\ \delta l_3 \end{pmatrix} = \begin{bmatrix} n_{1M2x} & n_{1M2y} & -n_{1M2x}c_{1y} \\ n_{1M2x} & n_{1M2y} & -n_{1M2x}c_{2y} \\ n_{3M2x} & n_{3M2y} & -n_{3M2x}c_{3y} \end{bmatrix} \begin{pmatrix} \delta x \\ \delta y \\ \delta \alpha \end{pmatrix} = M_{forw} \begin{pmatrix} \delta x \\ \delta y \\ \delta \alpha \end{pmatrix}. \quad (3)$$

The retrieval matrix can be calculated by a straightforward matrix inverse

$$M_{retr} = M_{forw}^{-1}. \quad (4)$$

## 5. TEST FACILITY CHARACTERIZATION

A characterization experiment is performed using the full thermal vacuum facility, where only the test object (OTA) is replaced by a zero length telescope. All other parts of the facility and setup are used. This test allows verification of the functionality of the setup, calibrate the thermal sensors, check the cleanliness of the facility and validate the accuracy of the metrology setup. The core idea behind the system test is that all aspects of the experiment are included, ranging from hardware to the test program itself. Any resulting deformation during this test is attributed to the setup and can be separated from the actual experiment performed on the test object. The performance of the setup is validated experimentally by running a full thermal test cycle encompassing a bake-out at +55°C, a number of deformation measurements up till -15°C and a warm up phase to 30°C to avoid dispositioning when going to ambient pressure. In preparation to this test a two-point calibration of the thermal sensors was performed by exposing a number of sensors consecutively to ice water and boiling water.

The overall test results showed that the deformations measured by the metrology system were below 50nm or 380nrad, and as such are within the required specification for defocus and tilt test tolerances of respectively 100 nm and 500 nrad. The latter are several orders below the expected deformations values, demonstrating the capabilities of the test setup to detect very small deformations of the integrated structure.

## 6. MEASUREMENT CAMPAIGN

A combined test program has been executed to validate the CHEOPS OTA STM structure, comprising various thermal aspects under investigation. The baseline temperature trajectory of the test is depicted in Figure 5 and consisted out of a bake-out at +55°C phase, deformation measurements for the stability settling case at +20°C and -10°C, the deformation measurements for the on-orbit stability case at -5°C, -10°C and -15°C and finally the warmup to ambient temperature and pressure. The order in which the set-point temperatures are depicted (green blocks) is followed during the test execution. Furthermore, to detect possible hysteresis inside the structure the temperature steps are included in the cooldown path as well as the warmup path. This thermal vacuum test program started on 9 September 2015 and lasted until 29 September 2015.

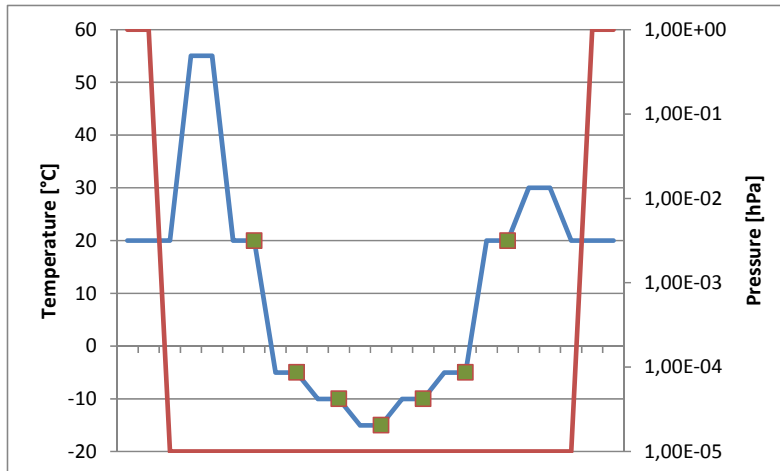


Figure 5. Schematic representation of test plan temperatures and pressure

## 7. TEST RESULTS

The key information that has to be retrieved from the test results is the relation between temperature and structural deformation. As a result of the test program an extensive data set is created, which needs to be processed in a number of steps to arrive at the test object deformation. First, taken a null reference point for the interferometers, which was at ambient temperature and high vacuum. Second, applied calibrated correction values to the temperature sensors. Figure 6 shows the interferometer data (left) and the temperature data (right) after these first two processing steps. Third, the IFM optical path length to mechanical deformation conversion has been executed as has been described in equations 1-4.

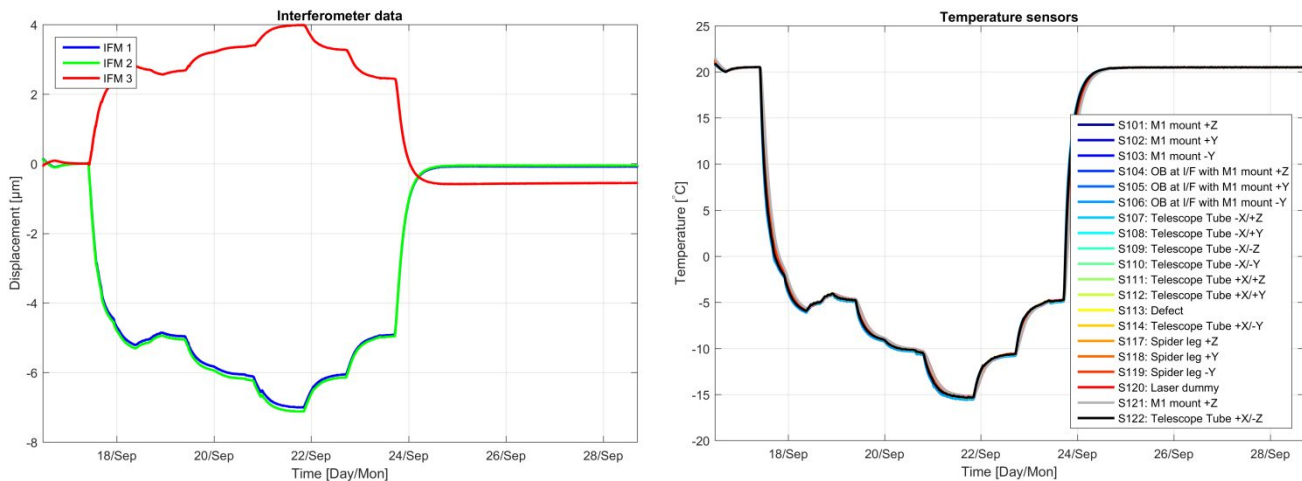


Figure 6. (Left) raw interferometer data, (right) test temperature profile.

Resulting deformation data over the experiment duration then is shown in Figure 7a, Figure 7b and Figure 7c; Transient temperature behavior gives a distorted image of the deformations, due to gradients inside the OTA structure. As such from the processed data the stable points as defined by the requirements are selected. These points are depicted with the red dots inside the figures and the temperatures and deformation values at these points are summarized in Table 1. This latter table is the final test result.

Table 1. Test result summary of STM test

Stabilization [°C]	Mean Temperature [°C]	$\Delta T$ temporal p-v [°C]	$\Delta T$ gradient p-v [°C]	Defocus $\delta x$ [ $\mu m$ ]	Decenter $\delta y$ [ $\mu m$ ]	tilt $\delta \alpha$ [ $\mu rad$ ]
+20/+21	20.5	0.04	0.12	0	0	0
-4/-5	-4.2	0.04	0.24	4.07	-2.2	-4.1
-10/-11	-10.4	0.07	0.45	5.18	-2.4	-5.9
-15/-16	-15.2	0.04	0.46	5.96	-2.7	-6.0
-10/-11	-10.7	0.02	0.29	5.09	-2.8	-4.3
-4/-5	-4.8	0.02	0.24	3.99	-2.8	-2.3
+20/+21	20.5	0.02	0.07	-0.27	-1.1	1.5

With respect to the set test requirements it is clear that the temperature temporal behavior is well below the required 0.5 K/hour and the 1 K /3 hour for respectively the on-orbit case and the settling case. Note that the presented values are over the applicable time windows. In addition, also the thermal gradient or homogeneity is with maximal 0.46K within the requested requirement of maximal 1K over the OTA-structure.

From the results we can also determine the test precision by looking at the noise levels of the deformation signals at stable operation points. For defocus, decenter and tilt this results in a  $\sigma$  of 1 nm, 22 nm and 104 nrad or in peak-valley values of 7 nm, 129 nm and 602 nrad. In combination with the earlier derived test tolerances during the test setup characterization of 50 nm and 380 nrad an accuracy of 51 nm, 72 nm and 484 nrad is achieved. Where the most stringent requirement was set for the on-orbit case with values for defocus and decenter of  $\pm 0.1 \mu m$  and tilt  $\pm 0.5 \mu rad$ . Which allows to conclude that the telescope structure thermal stability requirements were met.

Figure 7d depicts the relation between temperature and deformation which reveals that there is a difference between the cooldown and the warmup path. The difference for defocus, decenter and tilt is respectively  $-0.27 \mu m$ ,  $-1.1 \mu m$  and  $1.5 \mu rad$ . This can be caused by either a settling effect or by hysteresis. To distinguish between these two effects, a second consecutive test cycle would be required, which has not been performed.

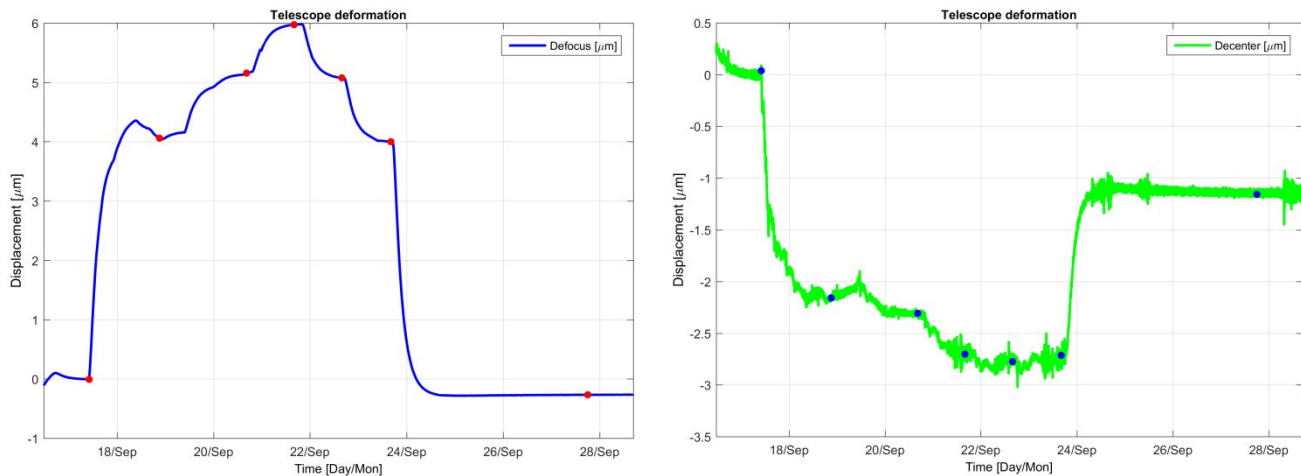


Figure 7. a) (top-left) Defocus deformation in relation to temperature, b) (top-right) decenter deformation in relation to temperature

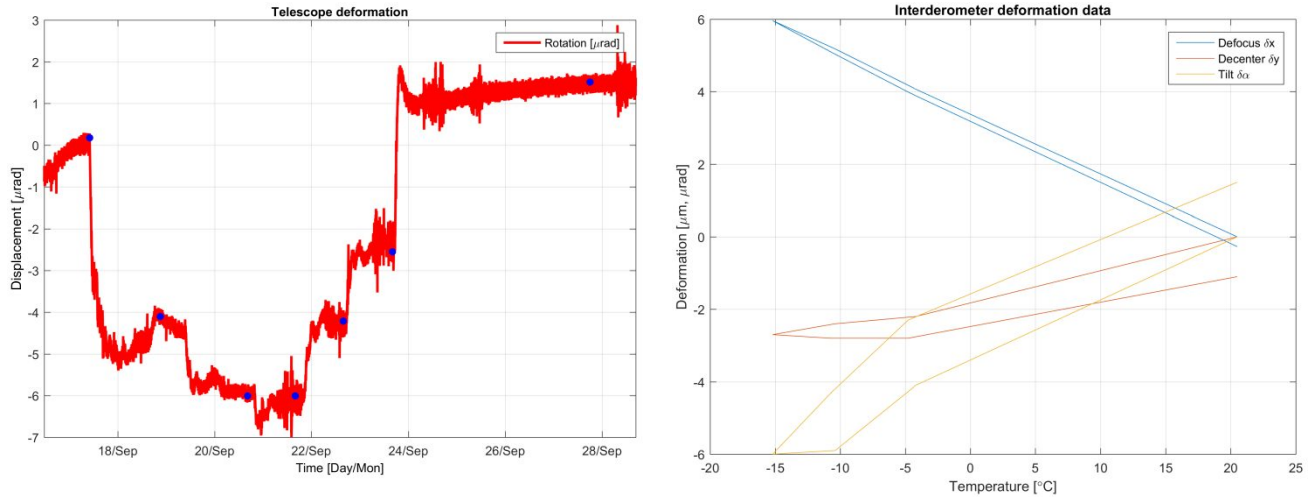


Figure 7. c) (bottom-left) rotation deformation in relation to temperature, d) (bottom-right) thermal deformation for the OTA structure

## 8. CONCLUSIONS & RECOMMENDATIONS

A successful experiment was performed on the CHEOPS Optical Telescope Assembly demonstrating the capabilities of the test setup as well as the realized thermal stability of the instrument. During a qualification experiment on a zero length telescope, the measurement accuracy of the integrated test setup was determined to be better than 50nm and 380nrad, well within the specifications, proving the validity of the measurement approach. Even more, the noise level of the measurement showed a standard deviation of respectively 1 nm, 22 nm and 104 nrad, which is several orders below the expected deformations of the telescope structure. This demonstrates the capabilities of the test setup to detect very small deformations of the integrated structure.

In the test campaign on the OTA structure deformations the various deformation requirements were tested to be within their specifications. Typical deformation numbers of the telescope being in the  $\mu\text{m}$  and  $\mu\text{rad}$  range over the operational temperature range. Our recommendation is that this data set can be used to assess the structure sensitivity to thermal gradients. Within the measurement campaign data was acquired continuously over time. Here the structure is specified and evaluated only under thermally stable and homogenous conditions. More detailed analysis of the intermediate data, where thermal gradients are present, is expected provide valuable feedback. Input can be derived for the determination of the required thermal insulation and thermal control on the telescope structure assembly.

In order to allow the distinction between hysteresis and settling effects, repetition of the thermal cycle is recommended. Here the settling effects are expected to occur only once where the hysteresis effects are predicted to repeat.

## ACKNOWLEDGEMENT

Most of the work presented in this paper has been performed under ESA contract N 4000110987/14 for the s-class CHEOPS mission under lead of the University of Bern. The telescope structure design is a joint effort of University of Bern and Almatech.

## REFERENCES

- [1] Benz., W. ,“CHEOPS – Characterising ExOPlanet Satellite Definition Study Report”, ESA/SRE(2013)7, November 2013
- [2] Verlaan, A.L., Lucarelli, S., Ende, D., “LISA Telescope Assembly Optical Stability Characterization for ESA”, Proceedings of the International Conference on Space Optics (ICSO), 2014